Article

Chaotic dynamics in a discrete-time predator-prey food chain

S. M. Sohel Rana

Department of Mathematics, University of Dhaka, Dhaka-1000, Bangladesh

E-mail: srana.mthdu@gmail.com

Received 4 November 2014; *Accepted 10 December 2014*; *Published online 1 March 2015*

Abstract

In this paper, we consider a classical discrete-time food chain model describing predators-prey interaction. The Holling type I functional response is used as the uptake for both predators. The existence and local stability of fixed points of the discrete dynamical system are analyzed algebraically. Using growth rate of prey as the bifurcation parameter, it is shown that the system undergoes a flip and Hopf bifurcations around planer or interior fixed point. It has been found that the dynamical behavior of the model is very sensitive to the parameter values and the initial conditions. Numerical simulations not only illustrate the key points of analytical findings but also exhibit complex dynamical behaviors of the model, such as the phase portraits, cascade of period-doubling bifurcation and determine the effects of operating parameters of the model on its dynamics. The Lyapunov exponents are numerically computed to characterize the asymptotic stability of the system dynamic response and estimate the amount of chaos in the system.

Keywords discrete-time food chain; stability; Flip and Hopf bifurcations; Lyapunov exponents.

Computational Ecology and Software
ISSN 2220-721X
URL: http://www.iaees.org/publications/journals/ces/online-version.asp
RSS: http://www.iaees.org/publications/journals/ces/rss.xml
E-mail: ces@iaees.org
Editor-in-Chief: WenJun Zhang
Publisher: International Academy of Ecology and Environmental Sciences

1 Introduction

The dynamics of predator-prey interaction is the starting point for many variations (food chain, food web etc.) that yield more realistic biological and mathematical problems in population ecology. Predation is a direct interaction which occurs when individuals from one population derive their nourishment by capturing and ingesting individuals from another population. There are many articles devoted to the study of predator-prey interaction both from the experimental and the modeling point of view. It is well known the Lotka-Voltera predator-prey model is one of the fundamental population models, a predator-prey interaction has been described firstly by two pioneers Lotka (1924) and Voltera (1926) in two independent works. After them, more realistic prey-predator model were introduced by Holling suggesting three types of functional responses for different species to model the phenomena of predation (Holling, 1965).

Qualitative analyses of prey-predator models describe by set of differential equations were studied by

many authors (Brauer and Castillo, 2001; Chauvet et al., 2002; Hastings and Powell, 1991; Klebanoff and Hastings, 1994; May, 1974; Murray, 1998; Zhu et al., 2002). Another possible way to understand a prey-predator interaction is by using discrete-time models. These models are more reasonable than the continuous time models when populations have non-overlapping generations (Brauer and Castillo, 2001; Murray, 1998) and lead to unpredictable dynamic behaviors from a biological point of view. This suggests the possibility that the governing laws of ecological systems may be relatively simple and therefore discoverable. The author (May, 1975, 1976) had clearly documented the rich array of dynamic behavior possible in simple discrete-time models. Recently, there is a growing evidence showing that the dynamics of the discrete-time prey-predator models can present a much richer set of patterns than those observed in continuous-time models (Agiza et al., 2009; Danca et al., 1997; Elsadany, 2012; Hasan et al., 2012; He and Lai, 2011; Ivanchikov, 2012; Jing et al., 2002, 2004, 2006; Li, 1975; Liu, 2007; Zengyun, 2011; He and Li, 2014; He, 2011). However, there are few articles discussing the dynamical behaviors of predator-prey models, which include bifurcations and chaos phenomena for the discrete-time models. The authors (He, 2011; Jing, 2006; Liu, 2007; Zengyun, 2011) obtained the flip bifurcation by using the center manifold theorem and bifurcation theory. But in (Agiza et al., 2009; Danca et al., 1997; Elsadany, 2012), the authors only showed the flip bifurcation and Hopf bifurcation by using numerical simulations. The dynamics of a tri-trophic discrete-time food chain models that incorporate Holling type response functions have more complex behaviors. A simple discrete-time food chain model had been examined by (Elsadany, 2012) which was the extended works in (Danca et al., 1997). They showed the system with two predators and one prey exhibit that the predator feeds exclusively on the prey, the top predator feeds on the predator and the prey is of logistic growth. Several studies used bifurcation analysis to find out if coexistence of all trophic levels is possible. In this paper, we are going to examine the dynamics of a discrete-time food chain where the top predator feeds exclusively on the prey and on the predator, the predator consumes the prey and the prey grows logistically in the absence of predators. The Holling type I functional response is used for both predators. In this work, we confine our interest to present, by using both analytic and numerical methods, the domains of the values of the parameters under which the system predicts that the populations will be able to persist at a steady state, the conditions for flip and/or Hopf bifurcations and the domain for the presence of chaos in the system by measuring the maximum Lyapunov exponents.

Our results in this paper are extension to those in (Danca et al., 1997; Elsadany, 2012). This paper is organized as follows. In Section 2, the classical discrete-time food chain model with Holling type I functional response is described. In section 3, we discuss the existence and local stability of fixed points for system (1) in R_+^3. In section 4, we present the numerical simulations which not only illustrate our results with theoretical analysis but also exhibit complex dynamical behaviors such as the cascade periodic-doubling bifurcation in periods 2, 4 and 8 and quasi-periodic orbits and chaotic sets. Finally a short discussion is given in Section 5.

2 The Model

In ecology, many species have no overlap between successive generations, and thus their population evolves in discrete-time steps (Murray, 1998). Such a population dynamics is described by difference equation. The discrete-time food chain we analyze in this paper consists of prey, predator and top predator. Let x_n denotes the number of prey population, y_n the number of predator population and z_n the number of top predator population in the nth generation. Our model is described by the following system of nonlinear difference equations in non-dimensional form:

$$H:\begin{cases} x_{n+1} = rx_n(1-x_n) - a_1x_ny_n - b_1x_nz_n \\ y_{n+1} = a_2x_ny_n - c_1y_nz_n \\ z_{n+1} = b_2x_nz_n + c_2y_nz_n \end{cases} \quad (1)$$

In the system (1), the prey, x grows logistically with intrinsic growth rate r and carrying capacity one in the absence of predation. The predator, y consumes the prey, x and the top predator, z consumes both the prey, x and predator, y with functional responses Holling type I. All parameters $r, a_1, a_2, b_1, b_2, c_1, c_2$ have positive values. From mathematical and biological point of view, we will pay attention on the dynamical behaviors of (1) in the first octant R_+^3. When all the species are present, the system is a simple food chain. In our model, when predator or top predator is omitted, the system reduces to a simple predator-prey interaction (Danca, 1997) and when the predation of top predator on prey is absent, it reduces to model (Elsadany 2012). Starting with initial population size (x_0, y_0, z_0), the iteration of system (1) is uniquely determined a trajectory of the states of population output in the following form

$(x_n, y_n, z_n) = H^n(x_0, y_0, z_0)$, where $n = 0,1,2,\cdots$.

3 The Fixed Points: Existence and Local Stability

In this section, we shall first discuss the existence of fixed points for (1), then study the stability of the fixed point by the eigenvalues for the Jacobian matrix of (1) at the fixed point.

It is clear that the system (1) has the following fixed points in the form $E(x, y, z)$:

$E_0(0,0,0)$: extinction of all populations.

$E_1\left(\frac{r-1}{r},0,0\right)$: survival of population x only.

$E_2\left(\frac{1}{a_2}, \frac{r(a_2-1)-a_2}{a_1a_2}, 0\right)$: survival of populations x and y only.

$E_3\left(\frac{1}{b_2}, 0, \frac{r(b_2-1)-b_2}{b_1b_2}\right)$: survival of populations x and z only.

$E_4(x^*, y^*, z^*)$: coexist of all populations, where

$x^* = \frac{(1-r)c_1c_2 + a_1c_1 - b_1c_2}{a_1b_2c_1 - a_2b_1c_2 - rc_1c_2}$, $y^* = \frac{1-b_2x^*}{c_2}$ and $z^* = \frac{a_2x^*-1}{c_1}$.

To discuss the existence of fixed points, we say that fixed points will not exist if any one of its components is

negative. The fixed point E_0 always exists. The existence condition for E_1 is $r>1$ and similarly $r>\frac{a_2}{a_2-1}$ and $r>\frac{b_2}{b_2-1}$ (or $a_2>\frac{r}{r-1}$ and $b_2>\frac{r}{r-1}$) for E_2 and E_3 respectively. Finally, the feasibility condition for the interior fixed point E^* is $\frac{1}{a_2}<x^*<\frac{1}{b_2}$.

In the next step, we will investigate the local stability of these fixed points by finding the modules of eigenvalues of the associated Jacobian matrices. The Jacobian matrix due to the linearization of (1) about an arbitrary fixed point $E(x,y,z)\in R_+^3$ is given by

$$J(E)=\begin{bmatrix} r(1-2x)-a_1y-b_1z & -a_1x & -b_1x \\ a_2y & a_2x-c_1z & -c_1y \\ b_2z & c_2z & b_2x+c_2y \end{bmatrix}.$$

Let $\Delta_1=\left(1+\frac{r}{2a_2}\right)^2-r$ and $\Delta_2=\left(1+\frac{r}{2b_2}\right)^2-r$.

It is straightforward to compute the eigenvalues of $J(E_0)$ and $J(E_1)$ and we can obtain the following propositions showing the local dynamics of E_0 and E_1 if they exist.

Proposition 1. The fixed point E_0 is a sink if $r<1$, E_0 is a saddle if $r>1$, and E_0 is non-hyperbolic if $r=1$.

Proposition 2. The fixed point E_1 exists if $r>1$ and there are at least four different topological types of E_1 for all permissible values of parameters.

(i) E_1 is a sink if $1<r<\min\left\{3,\frac{a_2}{a_2-1},\frac{b_2}{b_2-1}\right\}$;

(ii) E_1 is a source if $r>\max\left\{3,\frac{a_2}{a_2-1},\frac{b_2}{b_2-1}\right\}$;

(iii) E_1 is non-hyperbolic if $r=3$ *or* $r=\frac{a_2}{a_2-1}$ *or* $\frac{b_2}{b_2-1}$;

(iv) E_1 is a saddle for the other values of parameters except those values in (i)–(iii).

We can easily see that for a fixed point E_1 if $(r,a_1,a_2,b_1,b_2,c_1,c_2)\in FB_{E_1}$ where

$$FB_{E_1}=\left\{(r,a_1,a_2,b_1,b_2,c_1,c_2): r=3, a_2\neq\frac{r}{r-1}, b_2\neq\frac{r}{r-1}, r>1, a_1,a_2,b_1,b_2,c_1,c_2>0\right\},$$

then one of the eigenvalues of $J(E_1)$ is -1 and the others are neither 1 nor -1. Therefore, there may be flip bifurcation of the fixed point E_1 if r varies in the small neighborhood $r=3$ and $(r,a_1,a_2,b_1,b_2,c_1,c_2)\in FB_{E_1}$.

When E_2 exists, the Jacobian matrix at E_2 is given by

$$J(E_2)=\begin{bmatrix} 1-\frac{r}{a_2} & -\frac{a_1}{a_2} & -\frac{b_1}{a_2} \\ \frac{r(a_2-1)-a_2}{a_1} & 1 & \frac{c_1(a_2+r-a_2r)}{a_1a_2} \\ 0 & 0 & \frac{a_1b_2+c_2(a_2r-a_2-r)}{a_1a_2} \end{bmatrix}.$$

Therefore, the eigenvalues of $J(E_2)$ are

$$\lambda_{1,2}=1-\frac{r}{2a_2}\pm\sqrt{\Delta_1} \text{ and } \lambda_3=\frac{a_1b_2+c_2(a_2r-a_2-r)}{a_1a_2}.$$

It is easy to see that $\lambda_{1,2}$ satisfy the equation

$$\lambda^2+\alpha_1\lambda+\alpha_2=0$$

where $\alpha_1=-tr(M_1)=-2+\frac{r}{a_2}$, $\alpha_2=\det(M_1)=\frac{r(a_2-2)}{a_2}$ and

$$M_1=\begin{bmatrix} 1-\frac{r}{a_2} & -\frac{a_1}{a_2} \\ \frac{r(a_2-1)-a_2}{a_1} & 1 \end{bmatrix}.$$

Using Jury's criterion (Elaydi, 1996), we have necessary and sufficient condition for local stability of the fixed point E_2 which are given in the following proposition.

Proposition 3. When $r>\frac{a_2}{a_2-1}$, then system (1) has a planer fixed point E_2 and

(i) it is a sink if one of the following conditions holds:

(i.1) $\Delta_1\geq 0$, $r<\frac{a_1a_2-a_1b_2+a_2c_2}{c_2(a_2-1)}$ and $\frac{3r}{r+3}<a_2<\frac{2r}{r-1}$;

(i.2) $\Delta_1 < 0$, $r < \dfrac{a_1a_2 - a_1b_2 + a_2c_2}{c_2(a_2 - 1)}$ and $a_2 < \dfrac{2r}{r-1}$.

(ii) it is a source if one of the following conditions holds:

(ii.1) $\Delta_1 \geq 0$, $r > \dfrac{a_1a_2 - a_1b_2 + a_2c_2}{c_2(a_2 - 1)}$ and $a_2 > \max\left\{\dfrac{3r}{r+3}, \dfrac{2r}{r-1}\right\}$;

(ii.2) $\Delta_1 < 0$, $r > \dfrac{a_1a_2 - a_1b_2 + a_2c_2}{c_2(a_2 - 1)}$ and $a_2 > \dfrac{2r}{r-1}$.

(iii) it is non-hyperbolic if one of the following conditions holds:

(iii.1) $\Delta_1 \geq 0$ and either $r = \dfrac{a_1a_2 - a_1b_2 + a_2c_2}{c_2(a_2 - 1)}$ or $a_2 = \dfrac{3r}{r+3}$;

(iii.2) $\Delta_1 < 0$ and $a_2 = \dfrac{2r}{r-1}$.

(iv) it is a saddle for the other values of parameters except those values in (i)–(iii).

Following Jury's criterion, we can see that one of the eigenvalues of $J(E_2)$ is -1 and the others are neither 1 nor -1 if the term (iii.1) of Proposition 3 holds. Therefore, there may be flip bifurcation of the fixed point E_2 if r varies in the small neighborhood of FB_{E_2} where

$$FB_{E_2} = \left\{(r, a_1, a_2, b_1, b_2, c_1, c_2): r = \frac{3a_2}{3 - a_2}, r \neq \frac{a_1a_2 - a_1b_2 + a_2c_2}{c_2(a_2 - 1)}, \Delta_1 \geq 0, r > 1, a_1, a_2, b_1, b_2, c_1, c_2 > 0\right\}.$$

Also when the term (iii.2) of Proposition 3 holds, we can obtain that the eigenvalues of $J(E_2)$ are a pair of conjugate complex numbers with module one. The conditions in the term (iii.2) of Proposition 3 can be written as the following set:

$$HB_{E_2} = \left\{(r, a_1, a_2, b_1, b_2, c_1, c_2): r = \frac{a_2}{a_2 - 2}, r \neq \frac{a_1a_2 - a_1b_2 + a_2c_2}{c_2(a_2 - 1)}, \Delta_1 < 0, r > 1, a_1, a_2, b_1, b_2, c_1, c_2 > 0\right\}$$

and if the parameter r varies in the small neighborhood of HB_{E_2}; then the Hopf bifurcation will appear.

Similar algebraic computation for the fixed point E_3 shows the local behavior of system (1) around E_3 which has been stated in the next proposition

Proposition 4. When $r > \dfrac{b_2}{b_2 - 1}$, then system (1) has a planer fixed point E_3 and

(i) it is a sink if one of the following conditions holds:

(i.1) $\Delta_2 \geq 0$, $r < \dfrac{b_1b_2 - a_2b_1 - b_2c_1}{c_1(1-b_2)}$ and $\dfrac{3r}{r+3} < b_2 < \dfrac{2r}{r-1}$;

(i.2) $\Delta_2 < 0$, $r < \dfrac{b_1b_2 - a_2b_1 - b_2c_1}{c_1(1-b_2)}$ and $b_2 < \dfrac{2r}{r-1}$.

(ii) it is a source if one of the following conditions holds:

(ii.1) $\Delta_2 \geq 0$, $r > \dfrac{b_1b_2 - a_2b_1 - b_2c_1}{c_1(1-b_2)}$ and $b_2 > \max\left\{\dfrac{3r}{r+3}, \dfrac{2r}{r-1}\right\}$;

(ii.2) $\Delta_2 < 0$, $r > \dfrac{b_1b_2 - a_2b_1 - b_2c_1}{c_1(1-b_2)}$ and $b_2 > \dfrac{2r}{r-1}$.

(iii) it is non-hyperbolic if one of the following conditions holds:

(iii.1) $\Delta_2 \geq 0$ and either $r = \dfrac{b_1b_2 - a_2b_1 - b_2c_1}{c_1(1-b_2)}$ or $b_2 = \dfrac{3r}{r+3}$;

(iii.2) $\Delta_2 < 0$ and $b_2 = \dfrac{2r}{r-1}$.

(iv) it is a saddle for the other values of parameters except those values in (i)–(iii).

Following Jury's criterion, we can see that one of the eigenvalues of $J(E_3)$ is -1 and the others are neither 1 nor -1 if the term (iii.1) of Proposition 4 holds. Therefore, there may be flip bifurcation of the fixed point E_3 if r varies in the small neighborhood of FB_{E_3} where

$$FB_{E_3} = \left\{(r, a_1, a_2, b_1, b_2, c_1, c_2): r = \frac{3b_2}{3-b_2}, r \neq \frac{b_1b_2 - a_2b_1 - b_2c_1}{c_1(1-b_2)}, \Delta_2 \geq 0, r > 1, a_1, a_2, b_1, b_2, c_1, c_2 > 0\right\}.$$

Also when the term (iii.2) of Proposition 4 holds, we can obtain that the eigenvalues of $J(E_3)$ are a pair of conjugate complex numbers with module one. The conditions in the term (iii.2) of Proposition 4 can be written as the following set:

$$HB_{E_3} = \left\{(r, a_1, a_2, b_1, b_2, c_1, c_2): r = \frac{b_2}{b_2-2}, r \neq \frac{b_1b_2 - a_2b_1 - b_2c_1}{c_1(1-b_2)}, \Delta_2 < 0, r > 1, a_1, a_2, b_1, b_2, c_1, c_2 > 0\right\}$$

and if the parameter r varies in the small neighborhood of HB_{E_3}; then the Hopf bifurcation will appear.

When the interior fixed point E_4 exists, the Jacobian matrix due to linearization of (1) about E_4 yields

$$J(E_4)=\begin{bmatrix} j_{11} & j_{12} & j_{13} \\ j_{21} & j_{22} & j_{23} \\ j_{31} & j_{32} & j_{33} \end{bmatrix}$$

where

$$j_{11}=\frac{a_1b_2c_1-a_2b_1c_2+r(b_1c_2-a_1c_1-2c_1c_2)+c_1c_2r^2}{a_1b_2c_1-a_2b_1c_2-c_1c_2r};\quad j_{12}=\frac{a_1(-a_1c_1+b_1c_2-c_1c_2+c_1c_2r)}{a_1b_2c_1-a_2b_1c_2+c_1c_2r};$$

$$j_{13}=\frac{b_1(-a_1c_1+b_1c_2-c_1c_2+c_1c_2r)}{a_1b_2c_1-a_2b_1c_2-c_1c_2r};\quad j_{21}=\frac{a_2(a_2b_1-b_1b_2+b_2c_1+c_1r-b_2c_1r)}{-a_1b_2c_1+a_2b_1c_2+c_1c_2r};\quad j_{22}=1;$$

$$j_{23}=\frac{c_1(-a_2b_1+b_1b_2-b_2c_1-c_1r+b_2c_1r)}{-a_1b_2c_1+a_2b_1c_2+c_1c_2r};\quad j_{31}=\frac{b_2(-a_1a_2+a_1b_2-a_2c_2-c_2r+a_2c_2r)}{-a_1b_2c_1+a_2b_1c_2+c_1c_2r};$$

$$j_{32}=\frac{c_2(-a_1a_2+a_1b_2-a_2c_2-c_2r+a_2c_2r)}{-a_1b_2c_1+a_2b_1c_2+c_1c_2r};\quad j_{33}=1;$$

and that the eigenvalues of $J(E_4)$ satisfy the equation

$$\lambda^3+\mu_1\lambda^2+\mu_2\lambda+\mu_3=0 \tag{2}$$

where

$$\begin{aligned}\mu_1&=-trace(J(E_4))=-(j_{11}+j_{22}+j_{33})\\ \mu_2&=j_{11}j_{22}-j_{12}j_{21}+j_{22}j_{33}-j_{23}j_{32}+j_{11}j_{33}-j_{13}j_{31}\\ \mu_3&=-\det(J(E_4))=j_{13}j_{22}j_{31}-j_{12}j_{23}j_{31}-j_{13}j_{21}j_{32}+j_{11}j_{23}j_{32}+j_{12}j_{21}j_{33}-j_{11}j_{22}j_{33}\end{aligned} \tag{3}$$

The conditions for asymptotic stability (the roots of (2) satisfy $|\lambda|<1$) of the interior fixed point E_4 are obtained in the following proposition.

Proposition 5. If $\frac{1}{a_2}<x^*<\frac{1}{b_2}$, then positive fixed point E_4 exists and it is a sink iff

$$1+\mu_1+\mu_2+\mu_3>0,\quad 1-\mu_1+\mu_2-\mu_3>0$$
$$3+\mu_1-\mu_2-3\mu_3>0,\quad 1-\mu_1\mu_3-\mu_2-\mu_3^2>0.$$

Otherwise, E_4 will be either source or saddle or non-hyperbolic and therefore, the system (1) can undergo a flip or Hopf bifurcation around it.

In order to obtain the desired Hopf bifurcation for $r=r^*$ (using r as a bifurcation real parameter) around E_4, the equation (2) must have a pair of conjugate complex root with module one. Clearly (2) will have two pure imaginary roots if and only if

$$\mu_1\mu_2 = \mu_3 \tag{4}$$

for some values of r, say $r = r^*$. Thus for $r = r^*$, we have

$$\left(\lambda^2 + \mu_2\right)\left(\lambda + \mu_1\right) = 0$$

which has three roots $\lambda_{1,2} = \pm i\sqrt{\mu_2}$ and $\lambda_3 = -\mu_1$.

Therefore, the system (1) undergoes a discrete Hopf bifurcation around E_4 if r varies in the small neighborhood of HB_{E_4} where

$$HB_{E_4} = \left\{\left(r, a_1, a_2, b_1, b_2, c_1, c_2\right): \mu_2 = 1, \mu_1 \neq \pm 1, r > 1, a_1, a_2, b_1, b_2, c_1, c_2 > 0\right\}.$$

4 Numerical Simulations

In this section, our aim is to present numerical simulations to illustrate the key results of theoretical findings, especially the bifurcation diagrams, phase portraits and Maximum Lyapunov exponents for system (1) around the planer and positive fixed points (E_2 and E_4) and show the new interesting complex dynamical behaviors. It is known that Maximum Lyapunov exponents quantify the exponential divergence of initially close state-space trajectories and frequently employ to identify a chaotic behaviour. We left the simulation works for other fixed points as they are simple and similar. We choose the growth rate of prey, r as the real bifurcation parameter (varied parameter) and other model parameters are as fixed parameters, otherwise stated. For showing the dynamics of the system (1) change, we use different sets of parameter values which are given in the followings.

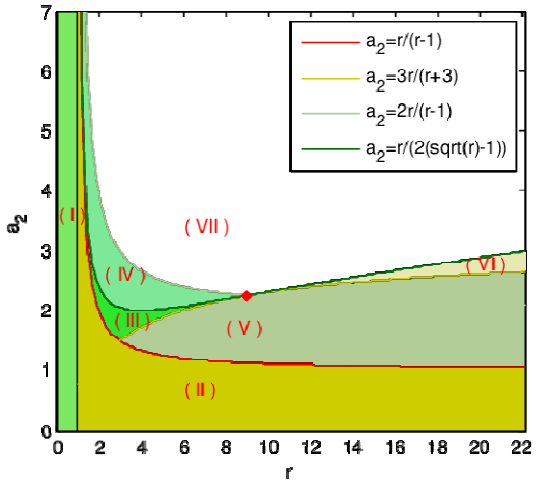

Fig. 1 Diagram of domains of the values of the parameters which correspond to different behaviors of the system.

4A Dynamics of system (1) around E_2

Before choosing the parameter values to see the complex (chaotic) behavior of system (1) around E_2, we present an operating diagram [in $(r - a_2)$ plane] in Fig. 1 of the domains of the values of parameters r and

a_2 which correspond to the conditions analytically established for the existence and stability of fixed point E_2 and for flip or Hopf bifurcations. We note that the values of the other parameter determine only the position of the fixed point in the phase plane. The curve $a_2 = r/(r-1)$ represents the inferior limit of the domain of parameters for which the fixed point E_2 exists. The regions III and IV correspond to the asymptotic stability of E_2 only. The values of parameters r and a_2 on the separation curve $a_2 = 3r/(r+3)$ between regions III and V (on the curve $a_2 = 2r/(r-1)$ between regions IV and VII) for $r < 9$ shows that the system (1) undergoes a flip bifurcation (Hopf bifurcation). For $r > 4$ and arbitrary a_2, the phase trajectories of the system (1) may become infinite due to sensitivity of the choice of the initial conditions. Details of reduced system (1) when $z = 0$, we refer (Danca et al., 1997).

Now we choose the parameter values in the following two cases:

Case (i): $a_1 = 2.3, a_2 = 21/13, b_1 = 0.8, b_2 = 1.5, c_1 = 2.5, c_2 = 0.15$ fixing and varying r in range $2.5 \le r \le 4$.

Case (ii): $a_1 = 2.3, a_2 = 3.3, b_1 = 0.8, b_2 = 1.5, c_1 = 2.5, c_2 = 0.15$ fixing and varying r in range $2.2 \le r \le 3.9$.

For case (i). The bifurcation diagrams of system (1) in ($r - x - y$) space and in ($r - x$) pane are given in Fig. 2(a-b). After calculation for the fixed point E_2 of map (1), the flip bifurcation emerges from the fixed point $(13/21, 10/69, 0)$ at $r = 7/2$ and $(a_1, a_2, b_1, b_2, c_1, c_2) \in FB_{E_2}$. It shows the correctness of proposition 3. From Fig. 2(b), we see that the fixed point E_2 is stable for $r < 7/2$ and loses its stability at the flip bifurcation parameter value $r = 7/2$, we also observe that there is a cascade of bifurcations for $r > 7/2$. The maximum Lyapunov exponents corresponding to Fig. 2(b) are computed and plotted in Fig. 2(c), confirming the existence of the chaotic regions and period orbits in the parametric space.

For case (ii). The bifurcation diagrams of system (1) in the ($r - x - y$) space, the ($r - x$) plane and the ($r - y$) plane are given in Fig. 3(a-b-c). After calculation for the fixed point E_2 of map (1), the Hopf bifurcation emerges from the fixed point $(100/299, 10/33, 0)$ at $r = 33/13$ and $(a_1, a_2, b_1, b_2, c_1, c_2) \in HB_{E_2}$. It shows the correctness of proposition 3. From Fig. 3(b-c), we observe that the fixed point E_2 of map (1) is stable for $r < 33/13$ and loses its stability at $r = 33/13$ and an invariant circle appears when the parameter r exceeds $33/13$, we also observe that there are period-doubling phenomenons. The maximum Lyapunov exponents corresponding to Fig. 3(b-c) are computed and plotted in Fig. 3(d), confirming the existence of the chaotic regions and period orbits in the parametric space. From Fig. 3(d), we observe that some Lyapunov exponents are bigger than 0, some are smaller than 0, so there exist stable fixed points or stable period windows in the chaotic region. In general the positive Lyapunov exponent is considered to be one of the characteristics implying the existence of chaos. The bifurcation diagrams for x and y together with maximum Lyapunov exponents is presented in Fig. 3(e). Fig. 3(f) is the local amplification corresponding to Fig. 3(b) for $r \in [3.203, 3.594]$.

The phase portraits which are associated with Fig. 3(a) are disposed in Fig. 4, which clearly depicts the process of how a smooth invariant circle bifurcates from the stable fixed point $(10/33, 100/299, 0)$. When r exceeds $33/13$ there appears a circular curve enclosing the fixed point E_2, and its radius becomes larger with respect to the growth of r. When r increases at certain values, for example, at $r = 3.2268$, the circle disappears and a period-6orbits appears, and some cascades of period doubling bifurcations lead to chaos. From Fig. 4, we observe that as r increases there are period-6, period-11, period-9, quasi-periodic orbits and attracting chaotic sets. See that for $r = 3.8796$ & 3.8966, where the system is chaotic, is the value of

maximal Lyapunov exponent positive that confirm the existence of the chaotic sets.

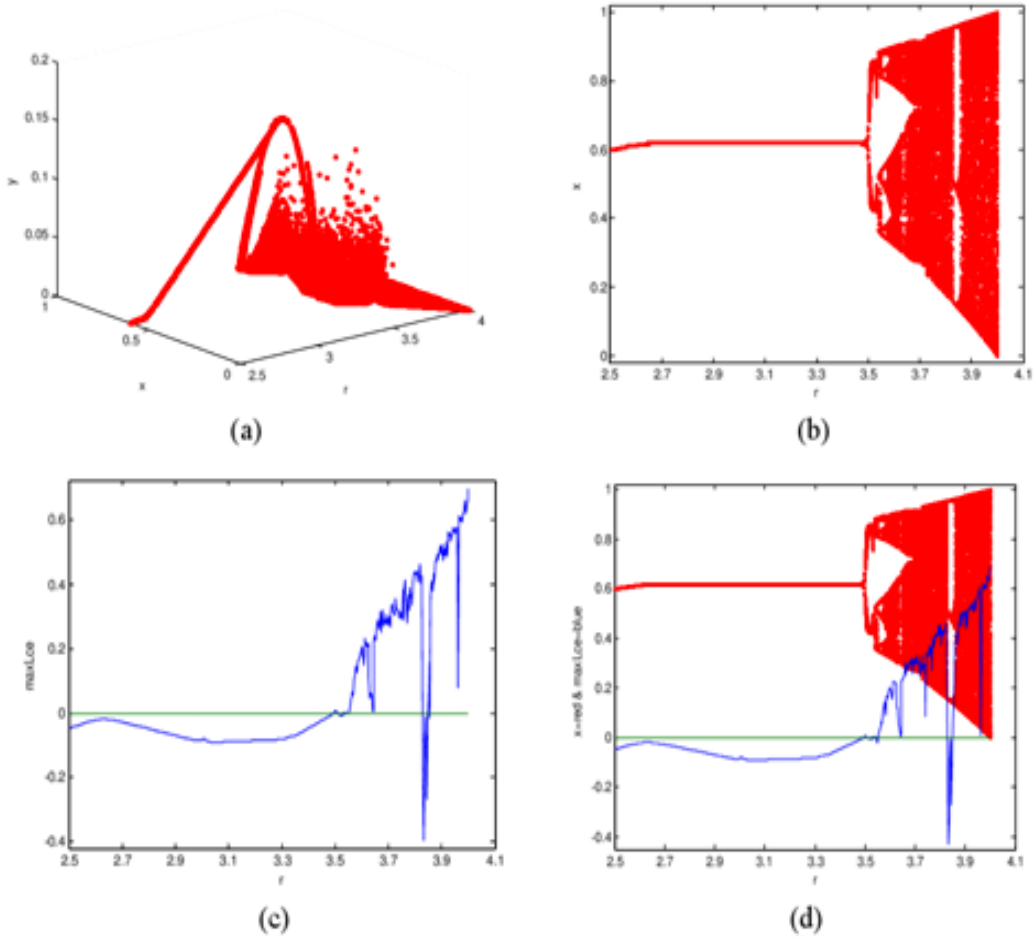

Fig. 2 Bifurcation diagrams and maximum Lyapunov exponent for system (1) around E_2. (a) Flip bifurcation diagram of system (1) in ($r-x-y$) space, the initial value is $(x_0, y_0, z_0) = (0.619, 0.145, 0.01)$ (b) Flip bifurcation diagram in ($r-x$) plane (c) Maximum Lyapunov exponents corresponding to (b) and (d) Maximum Lyapunov exponents are superimposed on Flip bifurcation diagram.

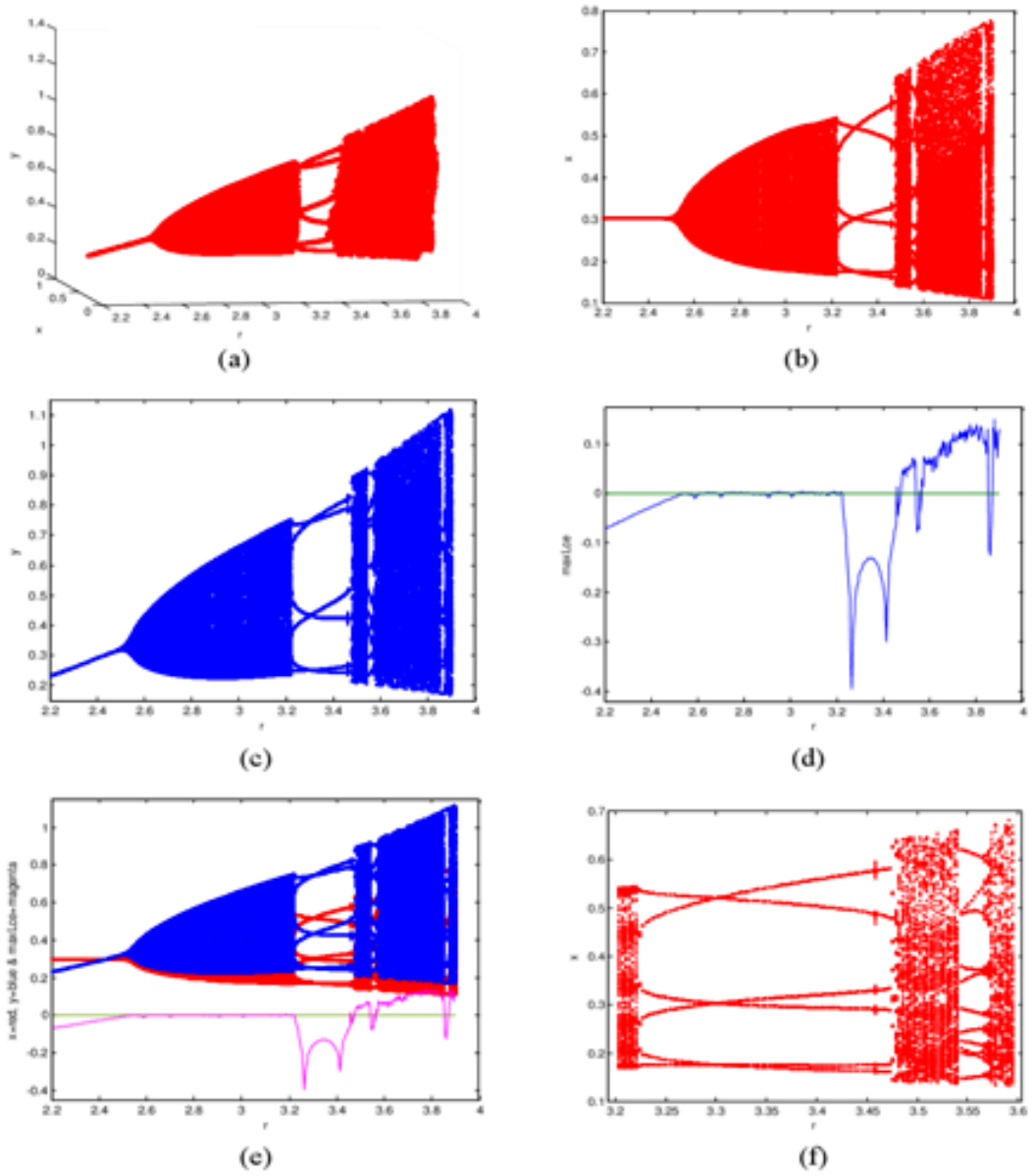

Fig. 3 Bifurcation diagrams and maximum Lyapunov exponent for system (1) around E_2. (a) Hopf bifurcation diagram of system (1) in ($r-x-y$) space (b-c) Hopf bifurcation diagrams in ($r-x$) and ($r-y$) planes (d) Maximum Lyapunov exponents corresponding to (b-c) (e) Maximum Lyapunov exponents are superimposed on bifurcation diagrams (f) Local amplification corresponding to (a) for $r \in [3.203, 3.594]$. The initial value is $(x_0, y_0, z_0) = (0.303, 0.334, 0.12)$.

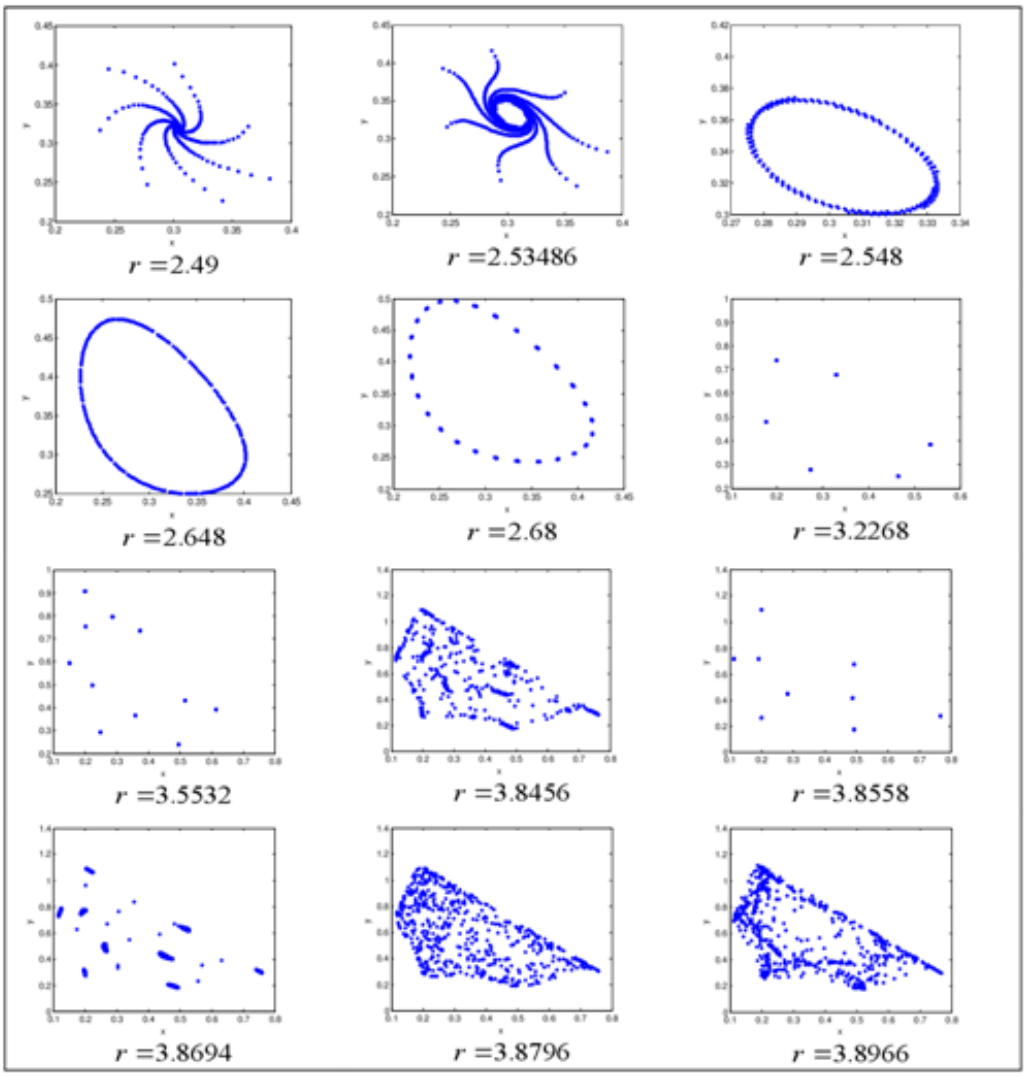

Fig. 4 Phase portraits for various values of r corresponding to Fig. 3(a).

In order to observe the complex dynamics, we can vary one more parameters of system (1). Since the values of Lyapunov exponents quantify the chaotic behavior of discrete system or at least sensitive dependence on initial conditions, so we compute maximum Lyapunov exponents of system (1) and study the dependence of these Lyapunov exponents on two real parameters r and a_2. The maximum Lyapunov exponents of system (1) for parameters $r \in [2.2,3.9]$ and $a_2 \in [1.6,3.3]$ and fixing other parameters as in case (ii) is given in Fig. 5(a). In Fig. 5(b) is plotted the sign of the maximal Lyapunov exponent of map (1). Blue color represents negative Lyapunov exponent and red color represents positive Lyapunov exponent. Here it is easy to see for which choice of parameters the system (1) is showing chaotic motion, and for which one is the system (1) exhibiting periodic or quasi periodic movement. E.g. the chaotic situation is on Fig. 4 for values of parameters $r = 3.8966$ & $a_2 = 3.3$ and the non-chaotic situation is for values of parameters $r = 3.2268$ & $a_2 = 3.3$ which are consistent with signs in Fig. 5(b).

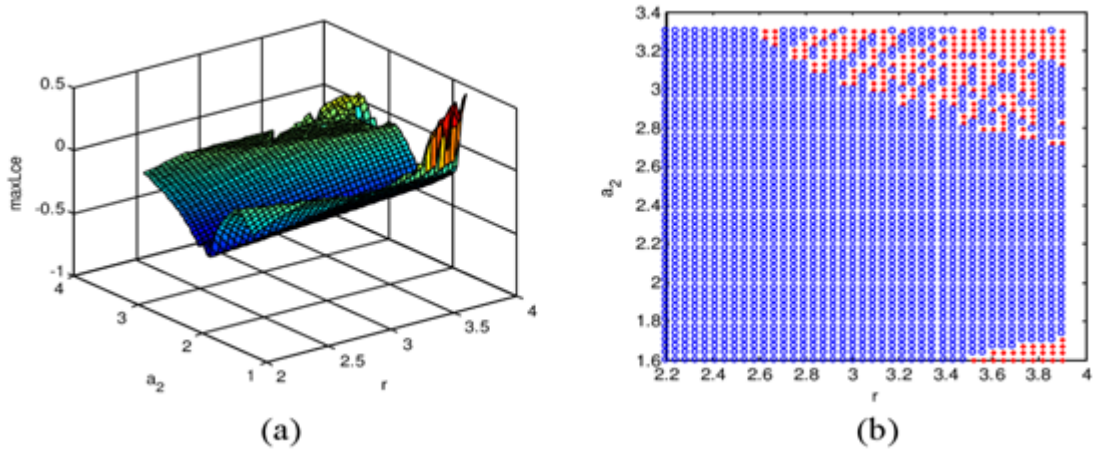

Fig. 5 Sign of maximum Lyapunov exponent for system (1) around E_2. (a) Maximum Lyapunov exponents of system (1) covering $r \in [2.2,3.9]$ and $a_2 \in [1.6,3.3]$ (b) Sign of Maximum Lyapunov exponents corresponding to (a) (red'*' = positive, blue'o' = negative). The initial value is $(x_0, y_0, z_0) = (0.619, 0.145, 0.01)$.

4B Dynamics of system (1) around E_4

The dynamic behaviors of the discrete system (1) around E_4 are very complex. To observe the dynamics, the parameters are considered in the following ways:

Case (iii): $a_1 = 3.2, a_2 = 2.0, b_1 = 1.8, b_2 = 1.33, c_1 = 3.5, c_2 = 3.0$ fixing and varying r in range $3.3 \le r \le 3.9$.

Case (iv): $a_1 = 3.7, a_2 = 3.0, b_1 = 0.09, b_2 = 0.03, c_1 = 3.5, c_2 = 3.8$ fixing and varying r in range $1.5 \le r \le 4.278$.

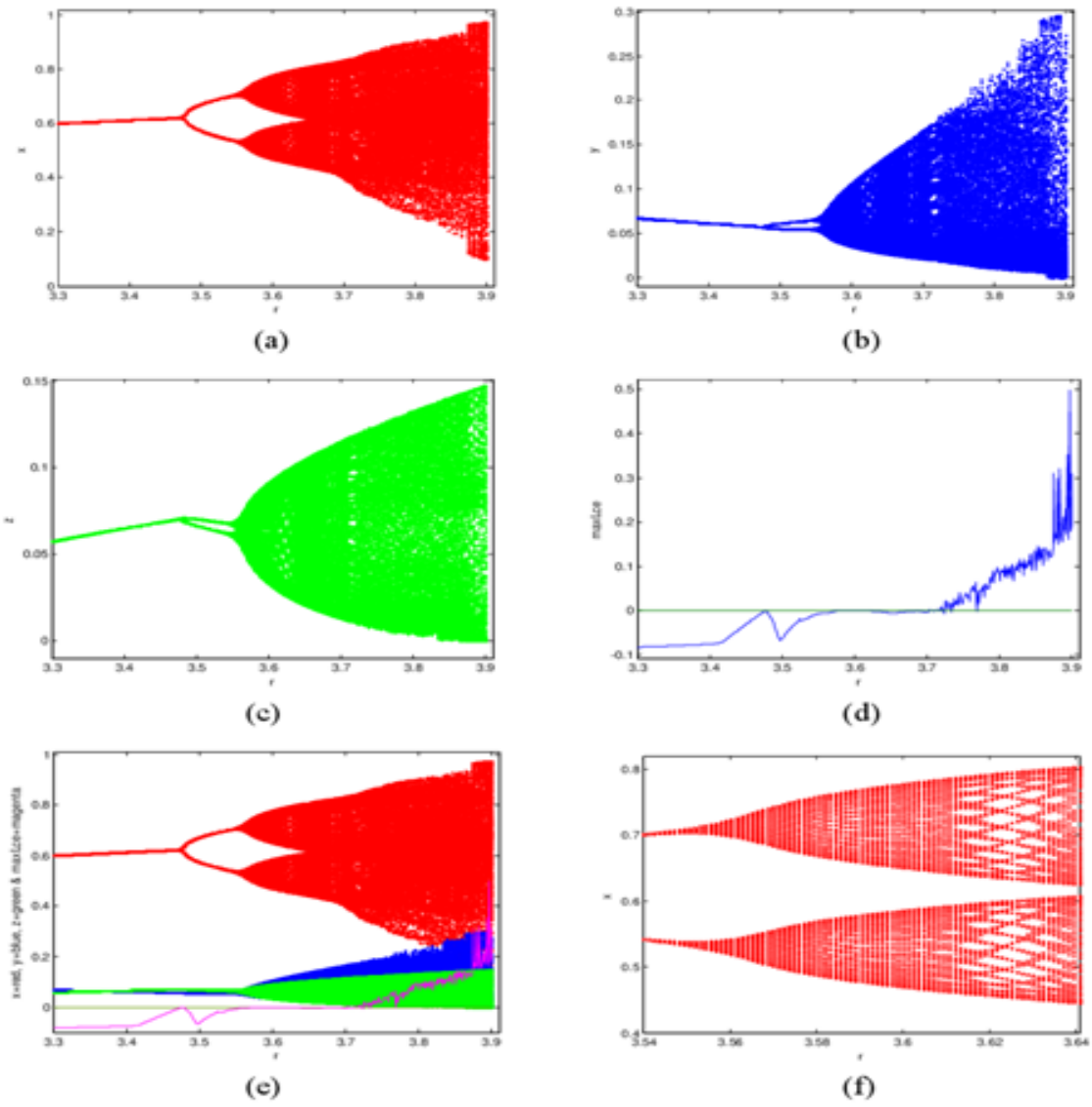

Fig. 6 Bifurcation diagrams and maximum Lyapunov exponent for system (1) around E_4. (a-c) Flip bifurcation diagram of system (1) with r covering [3.3,3.9], the initial value is $(x_0, y_0, z_0) = (0.63, 0.052, 0.076)$ (d) Maximum Lyapunov exponents corresponding to (a-c) (e) Maximum Lyapunov exponents are superimposed on bifurcation diagrams (f) Local amplification corresponding to (a) for $r \in [3.54, 3.641]$.

For case (iii). The bifurcation diagrams of system (1) in the ($r - x$), ($r - y$) and ($r - z$) planes are given in Fig. 6 (a-b-c). After calculation for the fixed point E_4 of map (1), the flip bifurcation emerges from the fixed point $(0.6234, 0.057, 0.0705)$ at $r = 3.476252$. From Fig. 6(a-b-c), we observe that the fixed point E_4 of map (1) loses its stability through a discrete flip bifurcation for $r \in [3.43, 3.479]$ and further increasing the parameter r, we see that there is a cascade of bifurcations. The maximum Lyapunov exponents corresponding to Fig. 6 (a-b-c) are computed and plotted in Fig. 6(d). The positive and negative values of Lyapunov exponents imply that there exist stable fixed points or stable period windows in the chaotic region. The combination of bifurcation diagrams with maximum Lyapunov exponents is presented in Fig. 6(e). Fig. 6(f) is the local amplification corresponding to Fig. 6(a) for $r \in [3.54, 3.641]$.

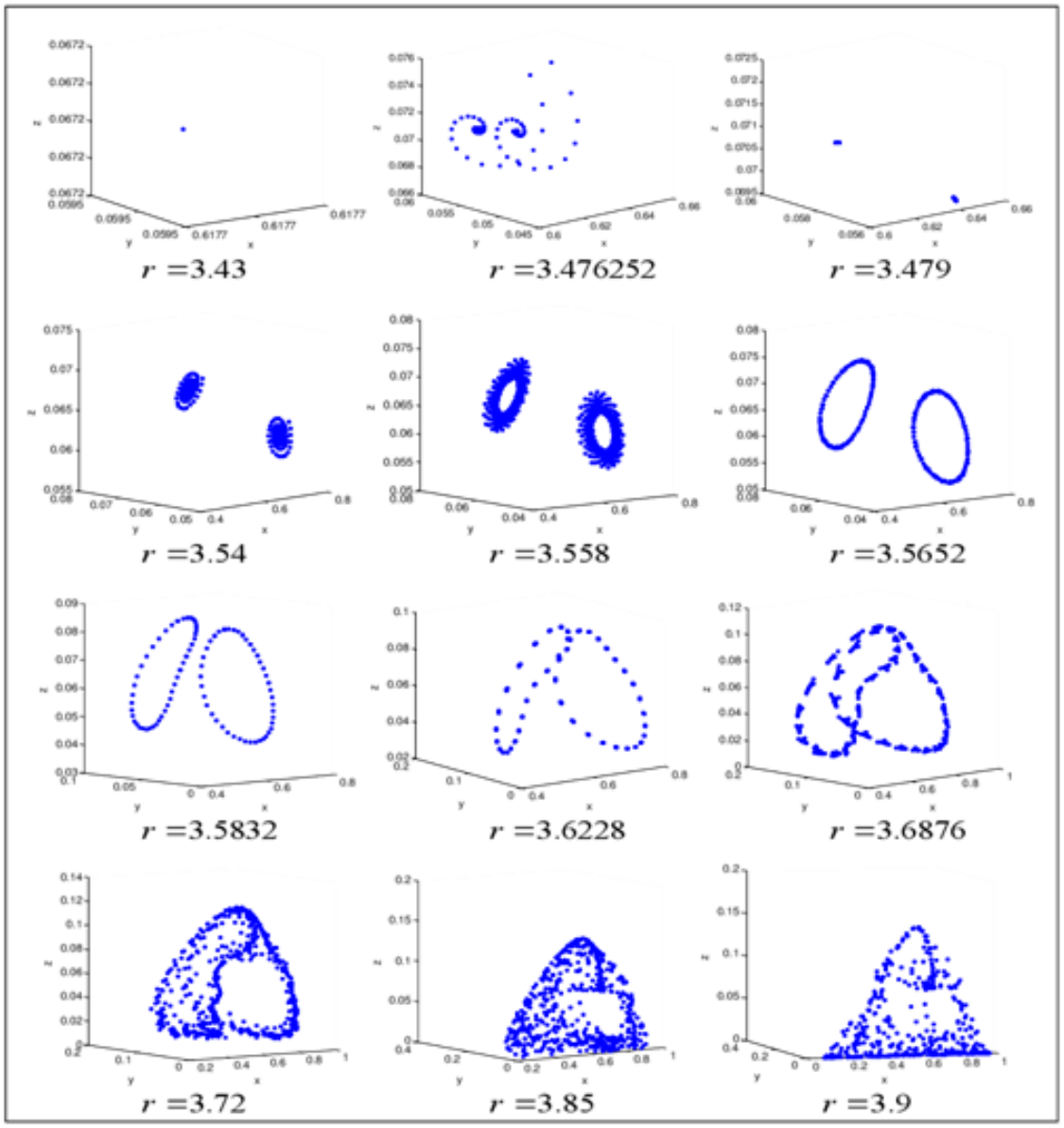

Fig. 7 Phase portraits for various values of r corresponding to Fig. 6(a-b-c).

The phase portraits which are associated with Fig. 6(a-b-c) are revealed in Fig. 7. We see that the fixed point E_4 loses its stability at the flip bifurcation parameter value $r = 3.476252$. For $r \in [3.54,3.5652]$, there is a cascade of bifurcations. When r increases at certain values, for example, at $r = 3.5652$, two independent invariant circles appear and increasing the value of r, the circles breakdown and some cascades of bifurcations lead to chaos. When $r = 3.85 \,\&\, 3.9$, we can see attracting chaotic sets. The maximum Lyapunov exponents corresponding to $r = 3.85 \,\&\, 3.9$ are larger than 0 that confirm the existence of the chaotic sets.

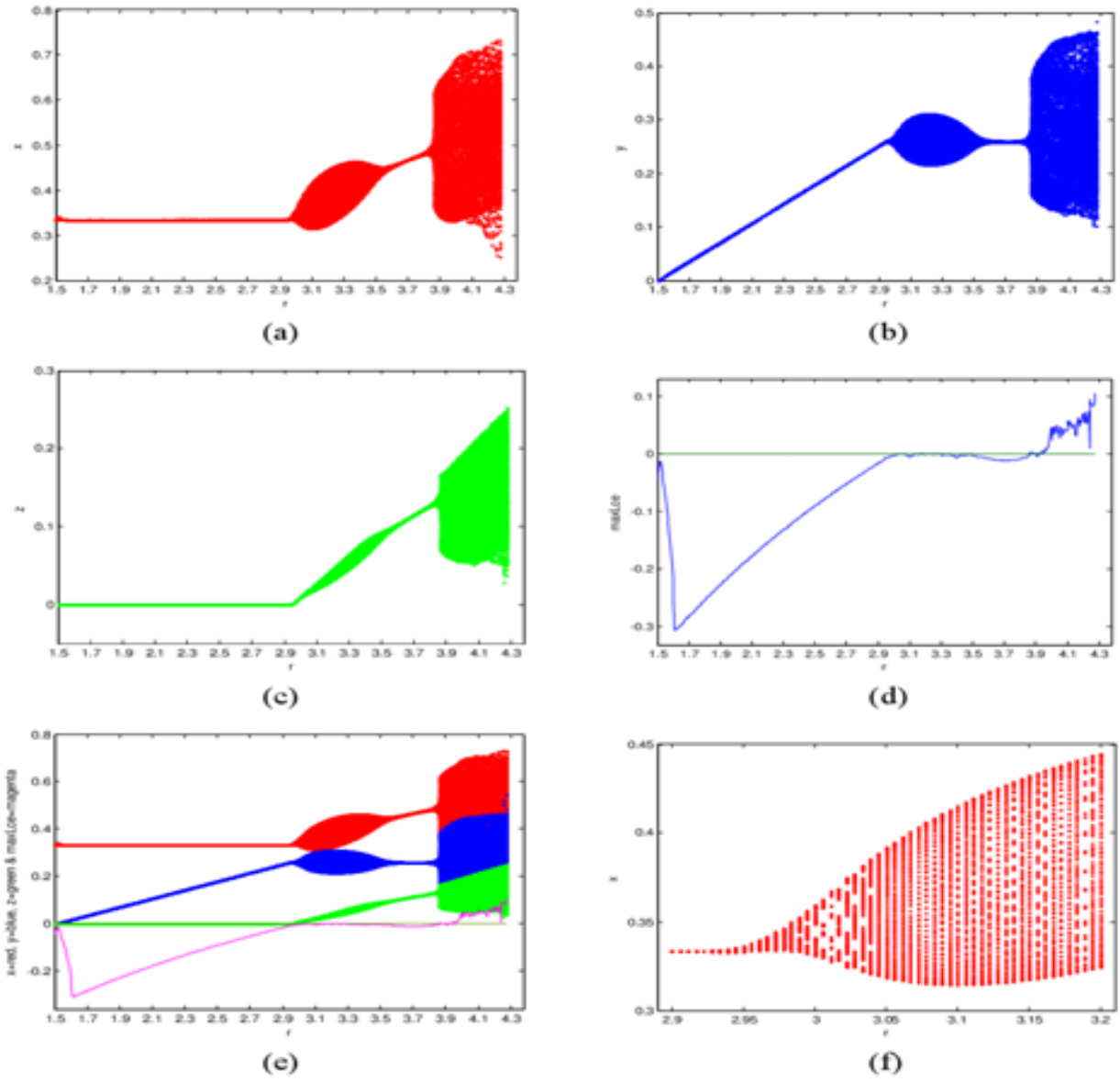

Fig. 8 Bifurcation diagrams and maximum Lyapunov exponent for system (1) around E_4. (a-b-c) Hopf bifurcation diagrams of system (1) with r covering $[1.5, 4.278]$, the initial value is $(x_0, y_0, z_0) = (0.33, 0.23, 0.05)$ (d) Maximum Lyapunov exponents corresponding to (a-b-c) (e) Maximum Lyapunov exponents are superimposed on bifurcation diagrams (f) Local amplification corresponding to (a) for $r \in [2.9, 3.2]$.

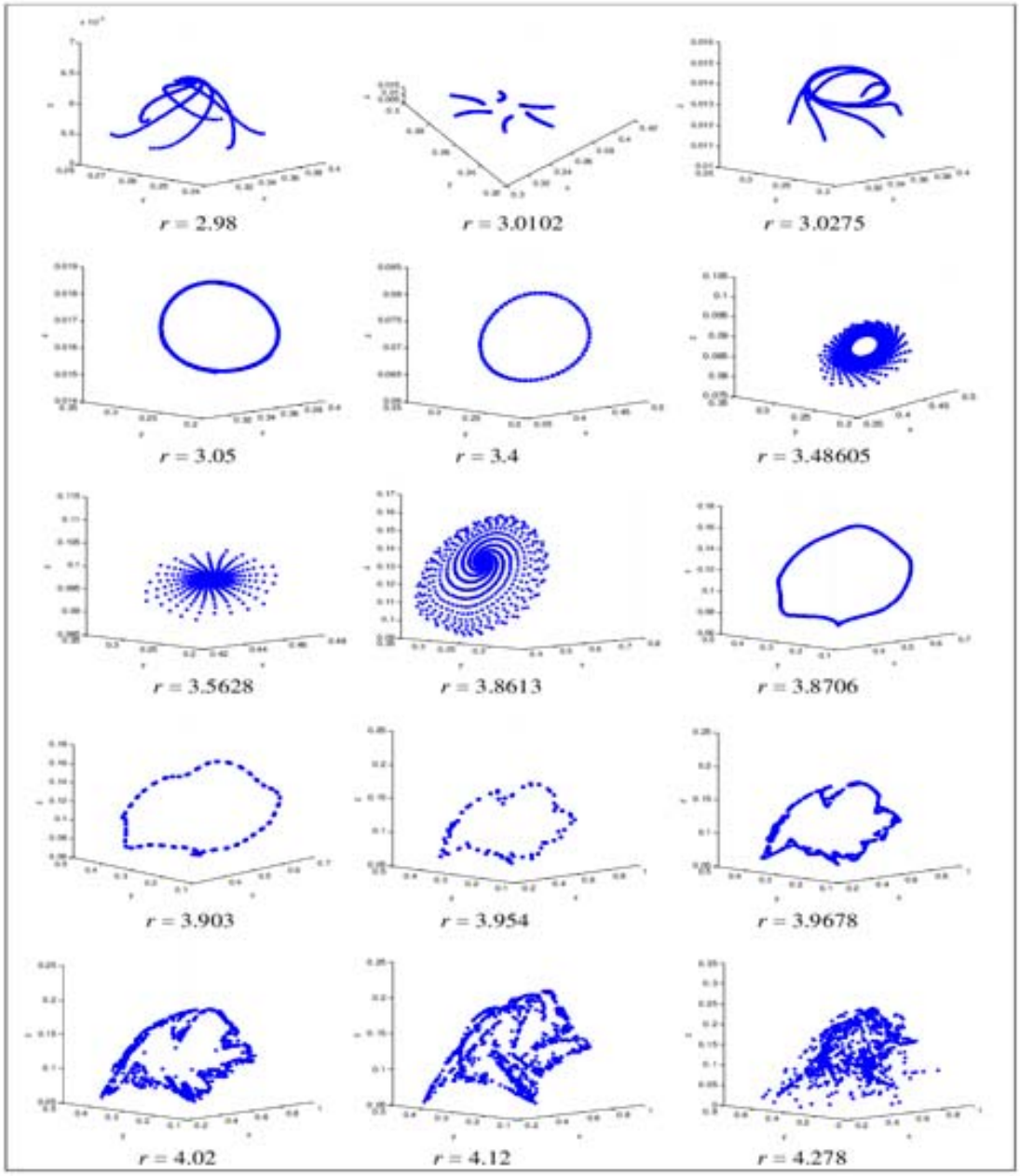

Fig. 9 Phase portraits for various values of r corresponding to Fig. 8 (a-b-c).

For case (iv). The bifurcation diagrams of system (1) in the $(r-x)$, $(r-y)$ and $(r-z)$ planes are drawn in Fig. 8(a-b-c). After calculation for the fixed point E_4 of map (1), the Hopf bifurcation emerges from the fixed point $(0.347,0.26,0.012)$ at $r=3.0102$ and $(a_1,a_2,b_1,b_2,c_1,c_2)\in HB_{E_4}$. From Fig. 8, we observe that the fixed point E_4 of map (1) is stable for $r<3.0102$; and loses its stability at $r=3.0102$ and an invariant circle appears when the parameter r exceeds 3.0102. The maximum Lyapunov exponents corresponding to Fig. 8(a-b-c) are computed and plotted in Fig. 8(d), confirming the existence of the chaotic regions and period orbits in the parametric space.For $r\in[2.98,3.5628]$, some Lyapunov exponents are bigger than 0, some are smaller than 0, which imply that there is a cascade of discrete Hopf bifurcations. For

$r > 3.9113$, the positive sign of maximum Lyapunov exponents indicate the presence of chaos of map (1).

The phase portraits of various r corresponding to Fig. 8(a-b-c) are disposed in Fig. 9, which clearly depicts the sequence of discrete Hopf bifurcation as the parameter r varies. When $r > 3.0102$, the first invariant circle appears at $r = 3.05$ enclosing the fixed point E_4. As r increases, the invariant circle breakdown and the map (1) enters into a discrete Hopf bifurcation around E_4 at $r = 3.48605$. For $r > 3.48605$, the fixed point of map (1) is stable again and it loses its stability at $r = 3.8613$. When r exceeds 3.8613 there appears a second invariant circle enclosing the fixed point E_4, and its radius becomes larger with respect to the growth of r. As r increases the phase trajectories become irregular which lead to attracting chaotic sets. At $r = 4.278$, we see that the system (1) is chaotic. The positive sign of maximal Lyapunov exponent corresponding to $r = 4.278$ confirms the existence of the chaotic sets.

5 Discussion

In this paper, we considered a classical discrete-time food chain model with Holling type I functional responses where the prey grows logistically in the absence of predators, the predator feeds on prey and the top predator feeds on both prey and predator. We performed a detailed computational analysis of the system (1) and showed that it has a complex dynamics in R_+^3. As certain parameters increase or decrease further away, we found that the fixed points (planer or interior) loses its stability and oscillatory solutions appear which is to be the results of flip bifurcation and/or Hopf bifurcation. Moreover, system (1) displayed much interesting dynamical behaviors, including period-6, 11, 9 orbits, invariant cycle, cascade of period-doubling, quasi-periodic orbits and the chaotic sets, which imply that the predators and prey can coexist in the stable period-n orbits and invariant cycle. Finally, simulation works showed that in certain regions of the parameter space, the model (1) had a great sensitivity to the choice of initial conditions and parameter values.

Acknowledgment

The author is thankful to the referees for their scrutiny.

References

Agiza HN, Elabbasy EM, EL-Metwally H, et al. 2009. Chaotic dynamics of a discrete prey-predator model with Holling type II. Nonlinear Analysis: Real World Applications, 10: 116-129

Brauer F, Castillo-Chavez C. 2001. Mathematical models in population biology and epidemiology. Springer-Verlag, New York, USA

Chauvet E, Paullet JE, Previte JP, et al. 2002. A Lotka-Volterra three-species food chain. Mathematics Magazine, 75: 243-255

Danca M, Codreanu S, Bako B. 1997. Detailed analysis of a nonlinear prey-predator model. Journal of Biological Physics, 23: 11-20

Elsadany AA. 2012. Dynamical complexities in a discrete-time food chain. Computational Ecology and Software, 2(2): 124-139

Elaydi SN. 1996. An Introduction to Difference Equations. Springer-Verlag, Netherlands

Hasan KA, Hama, M. F. 2012. Complex dynamics behaviors of a discrete prey-predator model with beddington-deangelis functional response. International Journal of Contemporary Mathematical Sciences,

7(45): 2179-2195

Hastings A, Powell T. 1991. Chaos in three-species food chain. Ecology, 72: 896-903

He ZM, Lai X. 2011. Bifurcations and chaotic behavior of a discrete-time predator-prey system. Nonlinear Analysis-Real World Applications, 12: 403-417

He ZM, Li B. 2014. Complex dynamic behavior of a discrete-time predator-prey system of Holling-III type. Advances in Difference Equations, 180

Ivanchikov PV, Nedorezov LV. 2012. About a modification of May model of parasite-host system dynamics Computational ecology and Software, 2(1): 42-52

Jing ZJ, Chang Y, Guo B. 2004. Bifurcation and chaos discrete FitzHugh- Nagumo system. Chaos, Solutions and Fractals, 21: 701-720

Jing ZJ, Yang J. 2006. Bifurcation and chaos discrete-time predator-prey system. Chaos, Solutions and Fractals, 27: 259-277

Jing ZJ, Jia Z, Wang R. 2002. Chaos behavior in the discrete BVP oscillator. International Journal of Bifurcation and Chaos, 12:619-627

Holling CS. 1965. The functional response of predator to prey density and its role in mimicry and population regulation. Memoirs of the Entomological Society of Canada, 45: 1-60

Klebanoff A, Hastings A. 1994. Chaos in three species food-chain. Journal of Mathematical Biology, 32: 427-245

Li TY, Yorke JA. 1975. Period three implies chaos. American Mathematical Monthly, 82: 985-992

Liu X, Xiao DM. 2007. Complex dynamic behaviors of a discrete-time predator prey system. Chaos, Solutions and Fractals, 32: 80-94

Lotka AJ. 1925. Elements of mathematical biology, Williams and Wilkins, Baltimore, USA

May RM. 1974. Stability and Complexity in Model Ecosystems. Princeton University Press, NJ, USA

May RM. 1975. Biological populations obeying difference equations: stable points, stable cycles and chaos. Journal of Theoretical Biology, 51(2): 511-524

May RM. 1976. Simple mathematical models with very complicated dynamics. Nature, 261: 459-467

Murray JD. 1998. Mathematical Biology. Springer-Verlag, Berlin, Germany

Volterra V. 1926. Variazioni e fluttuazioni del numero d'individui in specie animali conviventi, Mem. R. Accad. Naz. Dei Lincei, Ser. VI, Vol. 2

Zengyun Hu, Z. Teng, L. Zhang. 2011. Stability and bifurcation analysis of a discrete predator-prey model with nonmonotonic functional response, Nonlinear Analysis, 12(4): 2356-2377

Zhu H, Campbell SA, Wolkowicz G. 2002. Bifurcation analysis of a predator-prey system with nonmonotonic functional response. SIAM Journal on Applied Mathematics, 63: 636-682